

Effect of electroacoustic waves on radiation properties of microstrip matched coaxial termination

By A. M. SALEM, D. BHATNAGAR AND J. M. GANDHI

Microwave Laboratory, Department of Physics, University of Rajasthan,
Jaipur 302004, India

(Received 20 March 1995)

Expressions for the field intensities in a warm ionized plasma for two type of modes (electromagnetic and electroacoustic) pertaining to a microstrip matched coaxial termination are obtained using linearized hydrodynamic theory coupled with a vector function technique. The radiation power and directivity for the respective modes are evaluated for different ratios of plasma to source frequencies. It is observed that electromagnetic fields are similar to other microstrip antenna structures, but more directive in a particular direction. The electroacoustic mode exhibits a complete absence of multilobed structure, which was found for other antenna structures. The efficiency of this structure in a plasma is poor.

1. Introduction

For the past few years, printed circuit antennas have proven to be effective radiators because they are low-profile, extremely rugged and normally quite inexpensive to fabricate (Derneryd 1976; Carver & Mink 1981). They have found applications for communication in space (Post & Stephenson 1981).

Two widely used mathematical theories describing the plasma state involve the use of hydrodynamic theory coupled with a vector wave function technique and the Boltzmann equation in conjunction with the Maxwell equations. The use of the Boltzmann equation requires many assumptions, and hence hydrodynamic theory is used to study the radiation properties of a microstrip matched coaxial termination.

Mounted on a space vehicle, a radiator interacts with an isotropic, homogeneous, warm electron plasma, and produces two types of waves, namely transverse electromagnetic and longitudinal electroacoustic waves (Chen 1964).

The effect of electroacoustic waves on the radiation properties of the radiating element is investigated in this paper for a microstrip matched coaxial termination. The presence of dielectric polarization beneath the strip responsible for generation of a polarization current, in addition to the usual strip currents, is incorporated in the analysis of the radiated field (Abouzahra & Lewin 1979) in free space as well as in a plasma.

2. Basic assumptions and current distribution

The present analysis is carried out by considering the plasma as a isotropic, lossless, homogeneous, warm, non-drifting continuum of electrons and ions. For simplicity, the electrons are considered to be the effective component. Sheath formation around the antenna and the presence of an external magnetic field are disregarded. Under these simplifying assumptions, the electromagnetic and plasma fields are uncoupled, and can be separated into two independent modes, namely the electromagnetic and electroacoustic or plasma modes. It is considered here that only the aperture portion of the antenna encounters the plasma; this can be ensured by applying a protective layer ($d \leq 1$ mm) to the antenna structure. It is found that, with the application of a very thin protective layer, the fractional change in resonant frequency is about 0.7% at a resonant frequency of 1.2 GHz, which does not cause any serious change to the results.

The geometry of a microstrip matched coaxial termination is shown in figure 1. The width of the strip is W , the substrate thickness is h , and the substrate relative permittivity and permeability are $\epsilon_r > 1$ and $\mu_r = 1$ respectively. It is also assumed that the termination, which is a short post of height h , matches well with the strip and enters a matched coaxial line.

The radiation fields of the microstrip structure can be obtained by using different current conditions and distributions along the antenna structure. Similar far fields can be obtained either by considering electric and magnetic surface currents together, from a magnetic current density alone with a condition of perfect electrical conductivity, or from an electric current density alone with a condition of perfect magnetic current (Bahl & Bhartiya 1980).

In general, the current in a stripline fed at its end is

$$I_s = I_0(e^{-ik'z} - \Gamma e^{ik'z}),$$

where $k' = 2\pi\epsilon_{\text{eff}}^{1/2}/\lambda_0$ and Γ is the reflection coefficient at the end of the line. For a matched termination, $\Gamma = 0$. Hence the strip current is taken to be

$$I_s = I_0 e^{-ik'z}.$$

Assuming current amplitude to be constant across the strip line, the surface current density for an end-fed line is

$$\mathbf{J}_s = I_0 e^{-ik'z} e^{i\omega t} \hat{\mathbf{i}}_z.$$

A current of value unity is taken to flow in the negative x direction down the post.

In a microstrip antenna the wave, guided by the microstrip, remains concentrated under the strip and is incident on each aperture, where some power is radiated and the remainder is reflected back as a guided wave. Near the edges, there is some leakage of fields into the air above the strip. Dielectric polarization beneath the strip takes place, giving rise to a polarization current. The polarization current density is

$$\mathbf{J}_p = 2h \frac{\epsilon^* - 1}{\epsilon^*} \frac{\partial I_s}{\partial z} e^{i\omega t} \hat{\mathbf{i}}_x,$$

where ϵ^* is the actual dielectric constant.

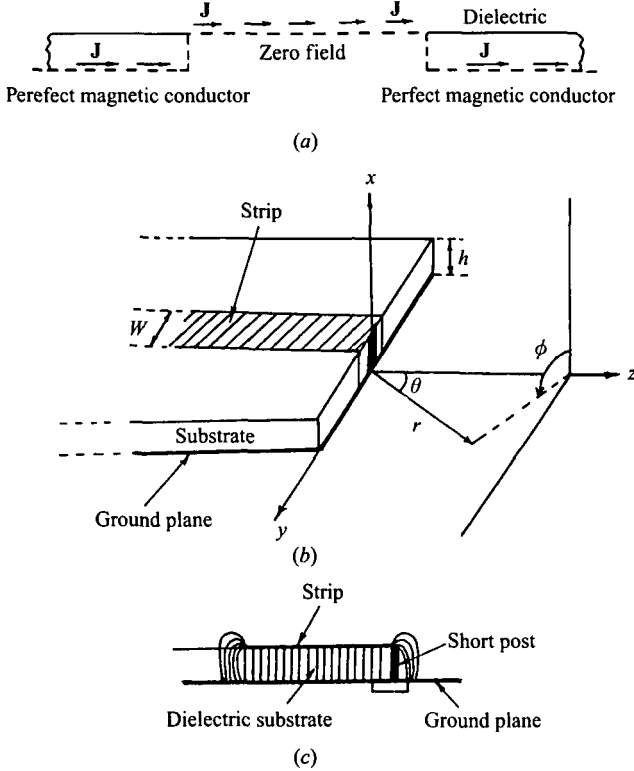


FIGURE 1. (a) Surface current source J alone plus a perfect magnetic conductor. (b) Antenna geometry with coordinate system. (c) Leakage of electric field into air.

For simplicity, the thickness of the dielectric substrate is taken to be much less than λ_0 (the wavelength in free space).

The contributions of both the strip current and the effective polarization current are considered simultaneously to obtain the radiation properties of a microstrip matched coaxial termination in free space as well as in plasma. When an antenna is surrounded by plasma, the effective permittivity of the structure changes marginally in comparison with that of free space (Schneider 1969); hence the resonant frequency also changes. It is predicted that the percentage change in ϵ_{eff} due to the plasma in comparison with free space is 0.018% for the antenna geometry under consideration. Hence the percentage deviation in frequency is about 0.003%, which is not very significant and will not cause serious changes to the results.

Considering the effect of the strip current and the effective polarization current together and following the method discussed in the appendix, expressions are obtained for the far-zone electromagnetic and electroacoustic components of the radiated field pattern. For the electromagnetic mode,

$$E_\theta = \frac{iZ_0 hW\beta_0 I_0 \epsilon^{\frac{1}{2}}}{2\pi r} \exp[i(\omega t - \beta_e r)] \frac{\cos \theta / \epsilon^* - \Lambda / \epsilon^{\frac{1}{2}}}{\epsilon - \Lambda \cos \theta} X_e \cos \phi, \quad (1)$$

$$E_\phi = \frac{iZ_0 hW\beta_0 I_0 \epsilon^{\frac{1}{2}}}{2\pi r} \exp[i(\omega t - \beta_e r)] \left(\frac{\epsilon^* - 1 / \epsilon^*}{\epsilon - \Lambda \cos \theta} - \frac{1}{\epsilon^{\frac{1}{2}}} \right) X_e \cos \phi, \quad (2)$$

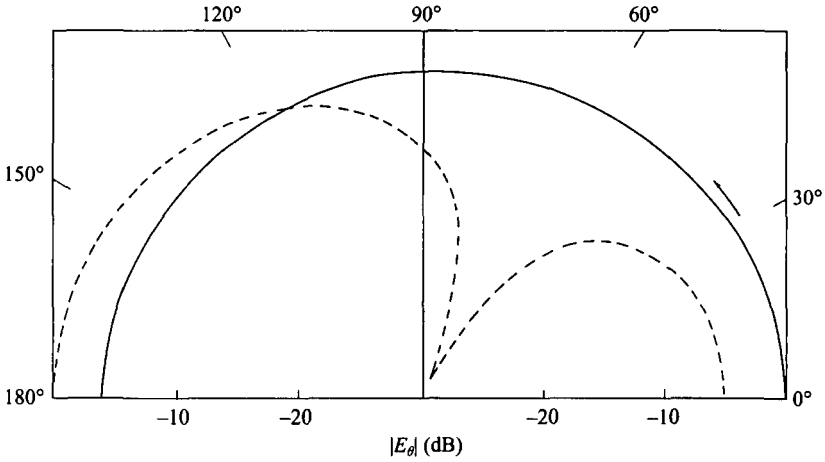


FIGURE 2. $|E_\theta|$ component of antenna for $\Lambda = 1$ (—) and 0.2 (---); $\theta = 0.001^\circ$.

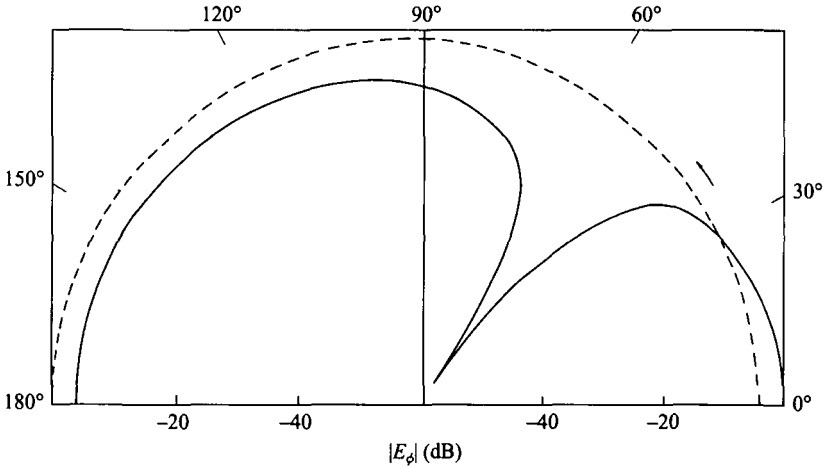


FIGURE 3. $|E_\phi|$ component of antenna for $\Lambda = 1$ (—) and 0.2 (---); $\phi = 0.001^\circ$.

where

$$X_e = \frac{\sin(\frac{1}{2}\beta_e W \sin \theta \sin \phi)}{\frac{1}{2}\beta_e W \sin \theta \sin \phi} \exp(i\frac{1}{2}\beta_e W \sin \theta \sin \phi),$$

$\beta_e = \Lambda \beta_0$, $Z_0 = 120 \pi$ and $\Lambda = (1 - \omega_p^2/\omega^2)^{\frac{1}{2}}$ is the plasma parameter. For the electroacoustic mode,

$$E_p = \frac{hW\omega_p^2\beta_p I_0}{2\pi r\omega(\omega^2 - \omega_p^2)\epsilon} \exp[i(\omega t - \beta_p r)] \\ \times \left\{ \left[\left(\epsilon^* - \frac{1}{\epsilon^*} \right) \frac{k'}{k' - \beta_p \cos \theta} - 1 \right] - \frac{\beta_p \sin \theta \cos \phi}{k' - \beta_p \cos \theta} \right\} X_p, \quad (3)$$

where

$$X_p = \frac{\sin(\frac{1}{2}\beta_p W \sin \theta \sin \phi)}{\frac{1}{2}\beta_p W \sin \theta \sin \phi} \exp(i\frac{1}{2}\beta_p W \sin \theta \sin \phi),$$

and $\beta_p = c\Lambda\beta_0/\nu$. Values of $|E_\theta|$, $|E_\phi|$ and $|E_p|$ are plotted in figures 2, 3, and 4

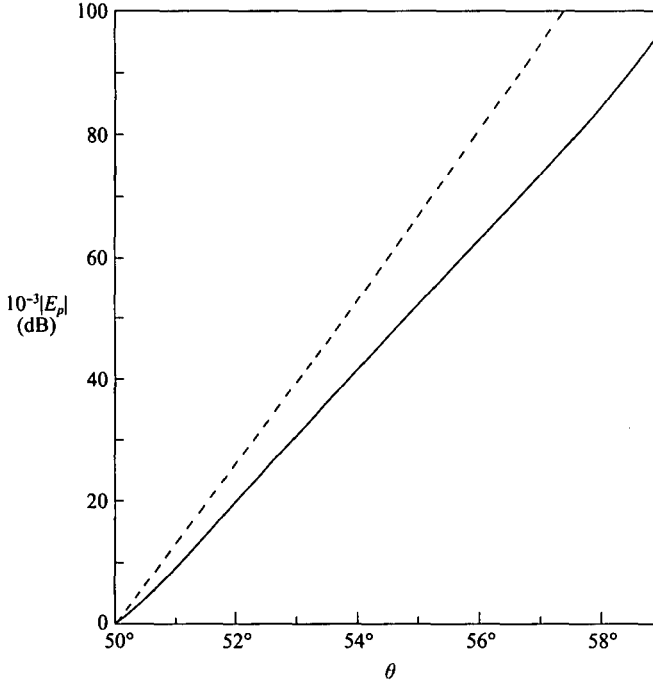


FIGURE 4. $|E_p|$ component of antenna for $\Lambda = 0.2$ (—) and 0.9 (---); $\phi = 90^\circ$.

respectively for different ratios of plasma to source frequencies. Note that here (and later in figures 5 and 6 and tables 1 and 2) values of $h = 0.158$ cm, $W = 0.471$ cm, $\epsilon = 2.31$, $\epsilon^* = 3.0$ and operational frequency 1.2 GHz have been used in the calculations.

The power radiated by an antenna in a plasma can be obtained by integrating the Poynting vector over a hemisphere. The total power radiated is the sum of the powers radiated in the electromagnetic and plasma modes.

2.1. Electromagnetic mode

The power radiated in this mode is

$$P_e = \frac{15\beta_0^2 h^2 W^2 \Lambda I_0^2 \epsilon}{\pi} \int_{-\frac{1}{2}\pi}^{\frac{1}{2}\pi} \int_0^\pi \left\{ \left[\frac{1}{\epsilon^{\frac{1}{2}}} - \frac{(\epsilon^* - 1)/\epsilon^*}{\epsilon^{\frac{1}{2}} - \Lambda \cos \theta} \right]^2 \sin^2 \phi + \left(\frac{\Lambda/\epsilon^{\frac{1}{2}} - \cos \theta/\epsilon^*}{\epsilon^{\frac{1}{2}} - \Lambda \cos \theta} \right)^2 \cos^2 \phi \right\} X_e^2 \sin \theta d\theta d\phi. \quad (4)$$

2.2. Electroacoustic mode

The power radiated in this mode is

$$P_p = \frac{mh^2 W^2 \omega_p^4 \beta_p I_0^2}{8\pi^2 \omega \epsilon^2 n_0 (\omega^2 - \omega_p^2)} \int_{-\frac{1}{2}\pi}^{\frac{1}{2}\pi} \int_0^\pi \left[\frac{\beta_p (\cos \theta - \sin \theta) - k'/\epsilon^*}{k' - \beta_p \cos \theta} \right]^2 \times X_p^2 \sin \theta d\theta d\phi, \quad (5)$$

where β_0 and β_p are the propagation constants of electromagnetic wave in free

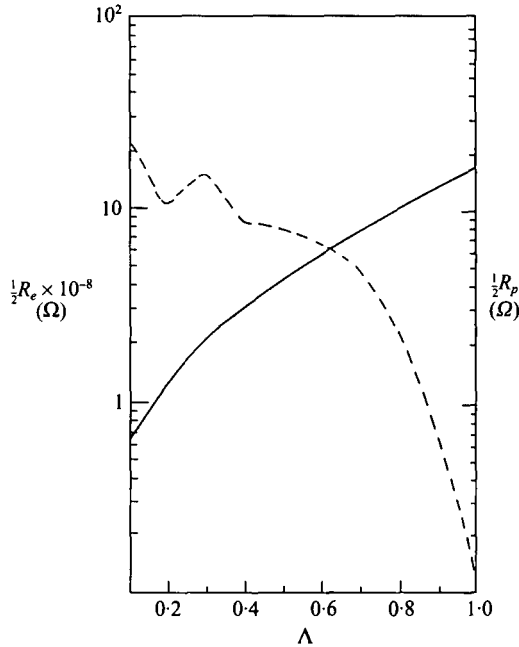


FIGURE 5. Radiation resistance in the electromagnetic and plasma modes: —, $R_e = 2P_e/I_0^2$; ---, $R_p = 2P_p/I_0^2$.

Plasma parameter Λ	Radiation resistance		Direction of maximum directivity		Directivity	
	$10^{-8} R_e$	R_p	EM mode	Plasma mode	$10^4 D_e$	$10^2 D_p$
0.1	12.53	439.67	180°	50°	1.36	4.04
0.2	26.27	204.62	180°	50°	1.57	4.16
0.3	42.47	300.24	180°	50°	1.70	1.82
0.4	62.36	170.86	180°	50°	1.74	2.10
0.5	87.25	160.02	180°	50°	1.73	1.54
0.6	118.45	124.28	180°	50°	1.63	1.47
0.7	157.36	100.01	180°	50°	1.61	1.26
0.8	205.67	44.86	180°	50°	1.50	1.70
0.9	265.08	14.81	0°	50°	1.67	2.33
1.0	337.83	0.00	0°	50°	3.24	—

TABLE 1. Radiation resistance, directivity and direction of maximum directivity for different values of Λ .

space and in plasma respectively, and ω_p is the angular plasma frequency of the electrons.

The power radiated in each of the two modes is calculated for different ratios of plasma to source frequencies and presented in figure 5.

With the help of (4) and (5), the radiation resistance of the antenna is calculated for different plasma parameter values, and is presented in table 1.

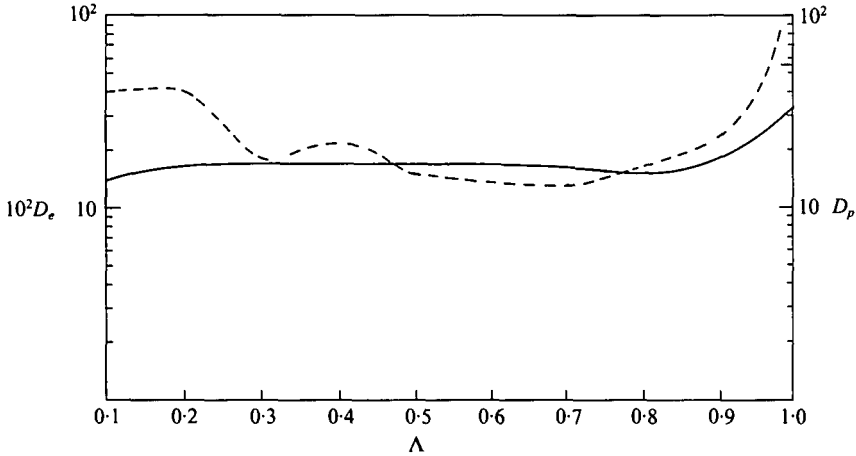


FIGURE 6. Directivity of antenna in the electromagnetic and plasma modes: —, D_e ; ---, D_p .

The directivity of an antenna is the value of the directive gain in the direction of its maximum. In the electromagnetic mode the directivity is

$$D_e = 4\pi \frac{F_{\max}(\theta, \phi)}{P_e},$$

where

$$F_{\max}(\theta, \phi) = [|E(\theta, \phi)|^2 + |E(\theta, \phi)|^2]_{\max}.$$

In the plasma mode

$$D_p = 4\pi \frac{|E_p(\theta, \phi)|_{\max}^2}{P_p}.$$

The directivity in each mode is calculated for different ratios of plasma to source frequencies, and is presented in figure 6.

The directions of maximum directivity (between 50° and 60°) and their respective values for the electromagnetic and plasma modes are presented in table 1 for different plasma parameter values.

3. Discussion and conclusions

The radiation properties of a microstrip matched coaxial termination in a warm lossless, homogeneous plasma have been studied. The $|E_\theta|$ pattern indicates that radiation pattern is almost uniform but the radiation intensity in the forward direction ($\phi = 0^\circ$) is slightly larger than that in the backward direction ($\phi = 180^\circ$). With a change in the ratio of plasma to source frequencies (from $\Lambda = 1.0$ to 0.2), the radiation pattern is drastically modified and becomes more directive in the forward direction. The 3 dB beamwidth in the forward direction is much smaller than that in the backward direction, as shown in Table 2.

On the other hand, the $|E_\phi|$ pattern has a lobe of large intensity and low 3 dB beamwidth in the $\theta = 0^\circ$ direction in free space. Furthermore it has a lobe of rather low intensity and large 3 dB beamwidth at $\theta = 180^\circ$. With changes in Λ , these patterns are modified to a great extent, and become almost uniform for low $\Lambda = 0.2$.

E_θ				E_ϕ			
Free space ($\Lambda = 1.0$)		Plasma ($\Lambda = 0.2$)		Free space ($\Lambda = 1.0$)		Plasma ($\Lambda = 0.2$)	
HPBW Front direction	HPBW Back direction	HPBW Front direction	HPBW Back direction	HPBW Front direction	HPBW Back direction	HPBW Front direction	HPBW Back direction
115°	122°	92°	112°	88°	120°	91°	122°

TABLE 2. Half-power beamwidth for $\Lambda = 1.0$ and 0.2 .

These variations in the $|E_\theta|$ and $|E_\phi|$ patterns are probably due to the fact that in a plasma, electroacoustic waves are excited in addition to electromagnetic waves. The $|E_p|$ pattern ($\phi = 89.99$) is very different in comparison with other microstrip structures (Bhatnagar and Gupta 1985*a, b*). Other structures have multilobed patterns. The radiation pattern in the present structure shows a complete absence of multilobed structure. Instead of this, a straight line is obtained. With increasing ratio of plasma to source frequencies, the slope of the line decreases. A multilobed pattern remains absent even in the range $\theta = 0-90^\circ$. Very close maxima and minima of small amplitude might well be present, but cannot be distinguished, giving the appearance of a straight line.

The power radiated by such a structure in the electromagnetic mode is a maximum in free space, but decreases with increasing ratio of plasma to source frequencies. The power radiated in the plasma mode increases with increasing ω_p/ω , and is much higher than that radiated in the electromagnetic mode. The useful power required for reception purposes is quite small, and the power going to waste in the form of plasma waves is very large. Therefore the radiation efficiency of such a structure in a plasma is extremely low; however, it can be used for reception purposes in free space.

For the electromagnetic mode, the directivity of this type of structure is maximum in free space, and marginally decreases with increasing ω_p/ω . For lower Λ , it remains almost unchanged. In the plasma mode the directivity does not show regular behaviour; however, it is much lower than that in the electromagnetic mode.

This study has revealed that the effect of a plasma on the radiation properties of a microstrip matched coaxial termination is quite significant and needs experimental varification, although production of the appropriate plasma medium under laboratory conditions is difficult.

The authors are grateful to CDPE, University of Rajasthan, Jaipur and to Dr A. K. Nagawat for providing computational facilities and other necessary help.

Appendix

The vector potential is

$$\mathbf{A} = \frac{\mu_0}{4\pi} \int_V \frac{\mathbf{J}(r)}{R} \exp(-i\beta_e R) dV. \quad (\text{A } 1)$$

For the strip line configuration, the integration with respect to dV is replaced by an integration over the cross-section and an integration with respect to dz . The strip current is

$$I_s = I_0 e^{-ik'z}. \quad (\text{A } 2)$$

Hence the strip current density is

$$\mathbf{J}_s = I_0 e^{-ik'z} e^{i\omega t} \hat{\mathbf{i}}_z. \quad (\text{A } 3)$$

Along with this, a current of unit value flows in the negative x direction down the coaxial line. The polarization current density is

$$\mathbf{J}_p = 2h \frac{\varepsilon^* - 1}{\varepsilon^*} \frac{\partial I_s}{\partial z} e^{i\omega t} \hat{\mathbf{i}}_x, \quad (\text{A } 4)$$

where I_s is a function of the feed-point location and the configuration of the strip line.

The far fields will be due to the strip current and the polarization current under the strip. On substituting \mathbf{J}_s and \mathbf{J}_p into (A 1) and simplifying, the vector potential becomes

$$\mathbf{A} = \frac{\mu_0 h W I_0}{2\pi r} \exp[i(\omega t - \beta_e r)] \left\{ \left[\frac{(\varepsilon^* - 1) \varepsilon^{\frac{1}{2}}}{\varepsilon^*(\varepsilon^{\frac{1}{2}} - \Lambda \cos \theta)} - 1 \right] \hat{\mathbf{x}} - \frac{\Lambda \sin \theta \cos \phi}{\varepsilon - \Lambda \cos \theta} \hat{\mathbf{z}} \right\} X_e. \quad (\text{A } 5)$$

The far-field components E_θ and E_ϕ can be obtained by using

$$E_\theta = \frac{Z_0}{\Lambda} H_{A\phi}, \quad E_\phi = \frac{-Z_0}{\Lambda} H_{A\theta}, \quad (\text{A } 6)$$

where

$$H_{A\phi} = \frac{1}{\mu_0} (\nabla \times \mathbf{A})_\phi, \quad H_{A\theta} = \frac{1}{\mu_0} (\nabla \times \mathbf{A})_\theta \quad (\text{A } 7)$$

On substituting (A 5) into (A 7) and hence into (A 6), equations (1) and (2) of the main text are obtained. Using the Poynting vector, the power radiated in the EM mode is obtained as

$$P = \frac{1}{2} \frac{\Lambda}{Z_0} \iint (|E_\theta|^2 + |E_\phi|^2) r^2 \sin \theta d\theta d\phi.$$

The plasma-mode radiation components can be obtained by calculating the total charge accumulated due to the strip current and the polarization current. Perturbation of the electron population density defined by a factor $n_1(r)$ can be written as

$$n_1(r) = \frac{1}{4\pi e\nu_0^2} \int \frac{\rho}{R} \exp(-i\beta_p R) dV, \quad (\text{A } 8)$$

where ρ is the accumulated charge on the radiator, ν_0 is the root mean square electron thermal velocity and β_p is as defined in the text.

The contributions from the charges accumulated due to the polarization and strip currents are calculated separately. Substituting $n_1(r)$ into the equation

$$E_p(r) = \frac{e\nu_0^2}{(\omega^2 - \omega_p^2) \varepsilon_0} \frac{\partial n_1}{\partial r}, \quad (\text{A } 9)$$

the Poynting vector in plasma mode is given by

$$S_p = \frac{1}{2} m \nu_0^2 n_1(r) V_p, \quad (\text{A } 10)$$

where V_p is the electron velocity vector. The radiated power in the plasma mode is obtained by integrating the Poynting vector over a hemisphere.

REFERENCES

- ABOUZAHRA, M. D. & LEWIN, L. 1979 Radiation from microstrip discontinuities. *IEEE Trans. Microwave Theory and Techniques* **27**, 722–723.
- BAHL, I. J. & BHARTIYA, P. 1980 *Microstrip Antennas*, pp. 5–10. Artech House, New York.
- BHATNAGAR, D. & GUPTA, R. K. 1985a Radiation from circular microstrip antenna in an ionized medium. *Indian J. Radio Space Phys.* **14**, 89–91.
- BHATNAGAR, D. & GUPTA, R. K. 1985b A comparative study of two new types of microstrip slot antennas in plasma medium. *Indian J. Radio Space Phys.* **14**, 113–116.
- CARVER, K. R. & MINK, J. W. 1981 Microwave antenna technology. *IEEE Trans. Antennas and Propagation* **29**, 1–24.
- CHEN, K. M. 1964 Interaction of a radiating source with a plasma. *Proc. IEE* **112**, 1668–1678.
- DERNERYD, A. G. 1976 Linearly polarized microstrip antenna. *IEEE Trans. Antennas and Propagation* **25**, 604–610.
- POST, R. E. & STEPHENSON, D. T. 1981 The design of a microstrip antenna array for a UHF space telemetry link. *IEEE Trans. Antennas and Propagation* **29**, 129–133.
- SCHNEIDER, M. V. 1969 *Bell Syst. Tech. J.* **48**, 1421–1444.